

Indoor Positioning Algorithm Comparison Based On A Multi-dimensional Fingerprint Dataset In Underground Parking

Ronghua Che

Liao cheng Infant Normal School, Computer Teaching and Research Office, Linqing City, Shandong Province ,252600

Abstract

Because of low cost and easy implementation, fingerprint based positioning algorithm is widely used in indoor positioning field. However, fingerprint dataset is easily affected by environment structure, equipment difference and signal frequency band. As underground parking becomes bigger and complex, the application demand of positioning is increasing. Unfortunately, there is no well-structured multi-dimensional open dataset for underground parking positioning. This paper selects part of the underground parking area of North China Electric Power University as the acquisition site, and divides the site into two acquisition areas according to the characteristics of areas, which are mainly roads or parking spaces. A month's multi-dimensional fingerprint dataset is collected. The dataset, organized weekly, is divided into four training sets and testing sets, its multi-dimension information consists of fingerprint acquisition point, time, temperature, humidity, acquisition direction, signal frequency band. After integrating and preprocessing the collected data, this paper analyzes the characteristics of the signals change, and uses the common positioning algorithms to carry out positioning experiments on the established datasets, and compares the positioning accuracy of different frequency bands.

Keywords

Indoor positioning; multi-dimensional datasets; WiFi fingerprint; underground parking.

1. Introduction

Position information plays an increasingly important role in the development of the information age^[1]. Due to the existence of Global Navigation Satellite System (GNSS), outdoor positioning has reached the centimeter-level positioning accuracy^[2]. However, in the indoor environment, GNSS is unreliable due to excessive signal attenuation. Therefore, for wireless positioning in indoor environment, a large number of studies have been carried out in the academic community to develop stable and accurate indoor positioning system (IPS). Some of these studies have achieved some results, such as Ultra Wideband (UWB) positioning^[3,4], Bluetooth positioning^[5], ultrasonic positioning^[6] and visible-light-based positioning methods^[7], but these schemes are limited in application potential due to the high cost of deploying additional equipment.

Compared with other algorithms, the indoor positioning method based on WiFi signal has become a hot topic in the current indoor positioning research due to the popularity of WiFi equipment^[8]. WiFi-based indoor positioning system can provide sufficient accurate position information to meet the application requirements such as store search, social networking, target advertising and user traffic analysis. Although WiFi positioning method has many advantages, there is no obvious successful WiFi-IPS business case in the market at present. The reasons behind include: (1) The standard to measure the positioning accuracy is not uniform; (2) Testing IPS in specific environments; (3) Testing IPS without considering signal stability.

These problems can be solved by different methods, for example, (1) Using a unified standard to measure the positioning accuracy^[9]; (2) Providing datasets of different environments^[10-12]; (3) Updating IPS training data^[13-15] regularly or make the positioning method adapt to signal changes^[16,17].

Since the WiFi signal fingerprint dataset in many studies (hereinafter referred to as 'datasets') is not public, the positioning results of the test on it are difficult to reproduce, which is not conducive to further research. Therefore, more and more researchers begin to pay attention to the establishment of public datasets^[12,18-22], and the reproducibility and comparability of indoor positioning research have been improved. However, there are still some shortcomings in the existing public datasets: (1) The acquisition cycle is short, the time interval is long, the acquisition area space is large, and the amount of data of the dataset is insufficient to reflect the real characteristics of signal changes; (2) The acquisition area is usually office environment or library, the environment structure is relatively fixed and single; (3) The acquisition data dimension is low, generally only including acquisition position coordinates, signal strength, acquisition time, and lack of environmental data. It can be said that the existing data acquisition regional environment structure is monotonous, the data dimension is low, and the amount of data is insufficient, which is difficult to meet the needs of indoor positioning research in different environments.

In underground parking, such as parking navigation, reverse car-seeking navigation and other applications, vehicle position information is required. However, the existing public dataset has a large difference between the positioning environment and the garage environment, which is not suitable for vehicle positioning research. At present, there is a lack of open multi-dimensional underground parking dataset with large amount of data and complete structure. Therefore, in order to meet the needs of underground parking positioning research, we choose the underground parking of a university as the acquisition area and establish the dataset. The fingerprint in the dataset consists of the signal strength of each Access Point (AP) in the collected environment, and the 10 fingerprint data collected in the same preset position and direction are a set of fingerprints. The dataset of underground parking is similar to the format of the dataset in [23]. According to the acquisition time, it is divided into different subsets, including WiFi received signal strength (RSS) data, position data and time data. At the same time, in order to analyze and compare the influence of environmental factors on positioning, this paper adds dimension data such as acquisition direction, acquisition signal frequency, AP position data, temperature and humidity of the environment.

The dataset established in this paper contains one month's data organized in weekly units, collected in two time periods every day. The acquisition samples, coordinates, measurement time, acquisition direction, signal frequency band and ambient temperature and humidity data of each acquisition point constitute different dimensions of WiFi signal fingerprint dataset, which is convenient to study the long-term and short-term RSS changes and the influence of different factors on positioning accuracy.

After establishing the dataset, this paper analyzes the relationship between the collected fingerprint data and the environmental structure of the underground parking by analyzing the variation characteristics of the signal RSS, and compares the influence of different signal frequency bands on the positioning accuracy. In addition, this paper uses six commonly used WiFi positioning methods to achieve positioning on the dataset in this paper, and analyzes and compares the positioning accuracy of different algorithms.

The division of the paper is as follows : Section 1 introduces the acquisition method and the environmental structure of the acquisition area in detail; Section 2 describes the meaning and organization form of data in the dataset; Section 3 analyzes the data characteristics of the dataset, and compares the positioning accuracy of the commonly used positioning methods on the dataset in this paper. Finally, the work is summarised in Section 4.

2. Data acquisition area and method

The data acquisition area of underground parking is a part of the underground parking of a university. Figure 1(a) is the actual scene of the underground parking. The area includes entrances, passageways and parking spaces for underground parking. The height is 2 m. Figure 1(b) shows the structure diagram of the acquisition area. The black solid dots in the figure represent the wireless network (i.e. AP) equipment in the acquisition area. Each AP equipment has two frequency bands of 2.4 GHz (referred to as 2.4 G) and 5 GHz (referred to as 5 G).

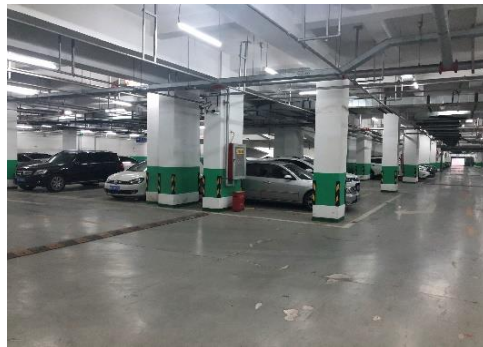


Figure 1(a) Scene map of underground parking

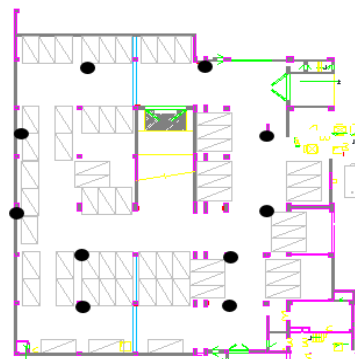


Figure 1(b) acquisition area structure

Data acquisition is completed by two trained personnel (hereinafter referred to as the 'collector'). The collectors stand in a predetermined position and use the computer placed on the trolley for data acquisition. The collectors use the WiFi signal acquisition software named NetSpot as Figure 2, and select the specified signal source (i.e. AP) for data acquisition. In the specified acquisition period, the collector must face a specific direction and collect data in order at each acquisition point. A set of fingerprint data is collected at each point, and the dimension data of environmental temperature and humidity are collected at the same time. The acquisition equipment is located at 1 m high in front of the collector. After the acquisition, the data of each dimension is organized into datasets according to the format described in section 2.

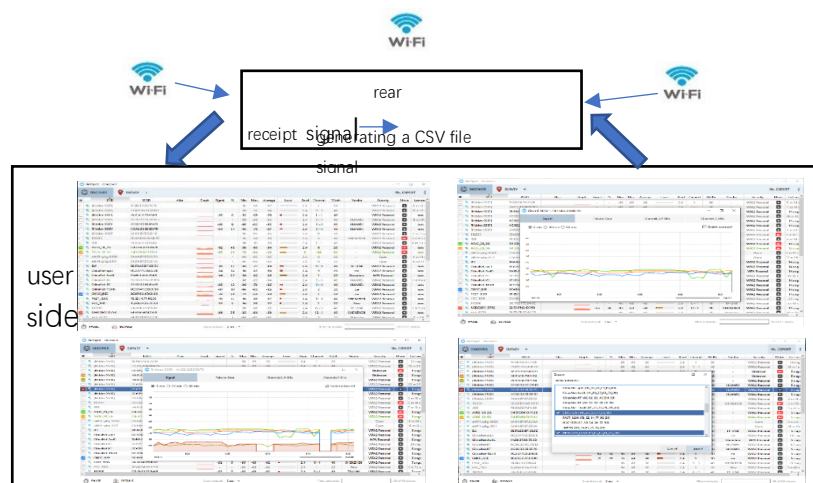


Figure 2 Signal acquisition software schematic

The acquisition area is divided into gate channel area (mainly roads) and parking area (mainly parking spaces) according to the environmental structure, and the dataset is divided into two categories. Then, according to the different acquisition time, the dataset is divided into four "acquisition week" datasets, and then divided into multiple testing sets and training sets according to the acquisition position. According to the distance between the parking spaces and the width of the road in the acquisition area, the distance between each Reference Point (RP)

in the training set is 2 m, and the distance between each RP in the testing set is 1 m. There are RPs of forward acquisition and reverse acquisition in both regions.

Figure 3 shows the position of RP in the gate channel area. The gate channel area surrounds the garage entrance, and the middle wall part forms a rectangular area where WiFi signal is difficult to pass, so the acquisition area can be regarded as a gate channel. In the three-layer portal RPs, the inner (pentagon, 41) and outer (solid semicircle, 45) layers are all training set RPs with a distance of 2 m. The middle layer is the testing set RPs, which are divided into four groups (22 solid triangles, 21 solid rectangles, 21 hollow triangles, and 21 hollow rectangles), with two adjacent RPs separated by 1 m and the same group of RPs separated by 4 m. The forward and reverse acquisition of the two types of datasets are carried out in different time periods. The forward acquisition sequence starts in the bottom right corner, advances along the direction of the arrow in the figure, and forms the "gate" trajectory, with the direction of the collector as the forward direction during the acquisition. The reverse acquisition starts in the bottom left corner, and the order is opposite to the forward acquisition.

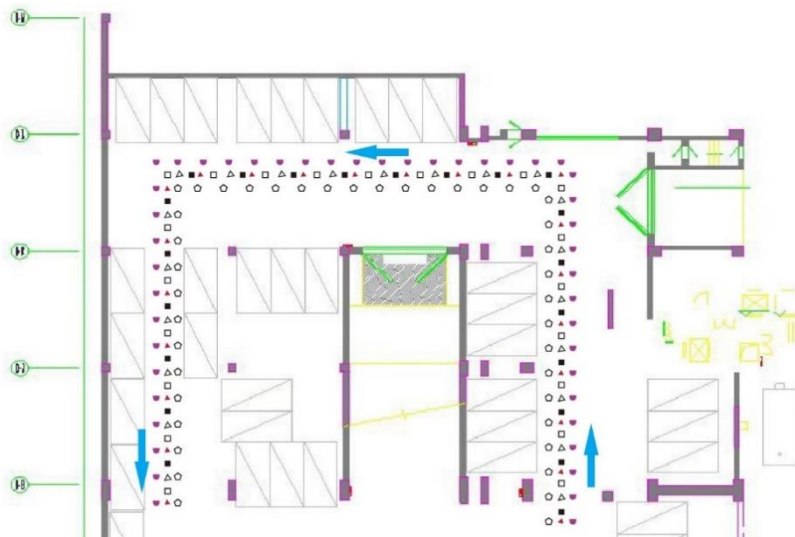


Figure 3 'gate' channel RP schematic

Figure 4 shows the RP position of the parking area, where the rectangle indicates the parking space. The top, middle and bottom three rows of hollow circles (a total of 39) are the training set RPs of the region, with RPs in the same row at a distance of 2 m. The other solid circles (56) are the testing set RPs of the region, located in a specific position in the region (such as the middle of the parking space). The acquisition process of the two datasets in this area is quite different, only the training set has carried out multi-directional acquisition at different times. In the training set, the forward acquisition starts from the RP in the bottom right corner, advances along the straight line in the direction of the arrow, and advances along the 'S' trajectory with the collector facing in the forward direction. The reverse acquisition starts from the RP in the top left corner, which is opposite to the direction of the forward acquisition process. The testing set RP is divided into two groups, one period to collect RPs in the parking space, and the other period to collect RPs not in the parking space. The orientation of the collector at the time of data acquisition is directly above in the map, and the RP selection in the parking space is determined by whether there is a car on the parking space at the time of acquisition.

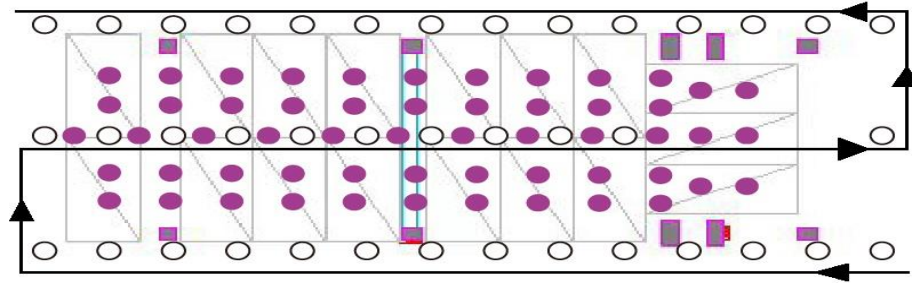


Figure 4 RP schematic of parking area

The acquisition area is 1210.74 m². The acquisition time of the testing set is 12:00-14:00 and 18:00-20:00 from Monday to Friday. The acquisition time of the training set is 6:00-8:00, 12:00-14:00 and 18:00-20:00 on Saturday and Sunday. Two collectors collect data in both areas at the same time.

3. Organization form of dataset

In this paper, 10 wireless routing devices are set up in the acquisition area, each device sends 2.4G and 5G band signals, and a total of 20 APs can be received. The dataset consists of 929 training set fingerprints and 1348 testing set fingerprints, with a total of 2277 fingerprints. Each fingerprint has 10 fingerprint vectors and the corresponding time, position and label vectors, the dataset contains 2277*10*4=91080 vector data.

The entire dataset DB is divided into two sub-datasets DB_i according to the acquisition area. Each DB_i contains four subsets $D_{\langle m,k,n \rangle}$ organized in weekly units. The dataset DB is defined as :

$$DB_i = \{D_{\langle m,k,n \rangle}\} \tag{1}$$

The i in the sub-dataset DB_i represents the region type of the dataset (1: gate channel area, 2: parking area). A data subset $D_{\langle m,k,n \rangle}$ represents the n th k -class dataset collected in the m th week. The subscript m denotes the week number of the acquisition. The dataset is collected for 4 weeks, and the value of m ranges from 1 to 4. The subscript k represents the type of dataset (1: training set, 2: testing set). The subscript n represents the number of dataset. In the training set, there is one training set in the gate channel area, and there are two training sets in the parking area, with the range of n from 1 to 2. In the testing set, RP is divided into two categories (forward and reverse) and four groups (such as four RPs in the middle layer of Figure 3) according to the position and direction of the gate channel area, with the range of n from 1 to 8. And the parking area is divided into eight groups according to the acquisition position and time. The range of n is also 1 to 8. Each data subset $D_{\langle m,k,n \rangle}$ contains four subsets : RSS subset $R_{(p \cdot s) \times a}$, location subset $L_{(p \cdot s) \times 3}$, time subset $T_{(p \cdot s) \times 1}$ and identifier subset $ID_{(p \cdot s) \times 1}$.

The RSS subset is composed of fingerprint vector groups collected at the same time period, which is defined as :

$$R_{(p \cdot s) \times a} = \{r_{i,j}\} \tag{2}$$

Among them, p denotes the number of RPs collected, s is the number of fingerprints collected by each RP ($s=10$), a is the number of APs received in the acquisition process ($a=20$), $r_{i,j}$ denotes the RSS value of the j -th AP (column) of the i -th fingerprint (row). If the AP signal is not received during acquisition, the corresponding $r_{i,j}$ values is '-', which is converted to -105 dBm in this dataset to participate in the positioning calculation. The value of p depends on the area and type of the dataset. The training set of the gate channel area is 860, the testing sets 1 and 2 are 220, and the testing sets 3, 4, 5, 6, 7, 8 are 210. The training set of the parking area is 780, and the testing set varies from 100 to 210.

The position subset is composed of the three-dimensional position coordinates of RP at acquisition, which is defined as :

$$L_{(p \cdot s) \times 3} = \{x_i, y_i, h_i\} \tag{3}$$

Among them, x_i, y_i are the two-dimensional coordinate system with the left lower corner of the underground parking lot as the origin, the coordinates corresponding to the i -th fingerprint. h_i is the height of the acquisition equipment from the underground parking ground, the value of h_i is 1 m.

Time subset consists of the collected time, defined as :

$$T_{(p \cdot s) \times 1} = \{t_i\} \tag{4}$$

t_i is the timestamp when collecting the i -th fingerprint. The timestamps are stored in the specified format and each timestamp is accurate to milliseconds. For example, the timestamp "201910191237666" indicates that the fingerprint was collected at 666 milliseconds on 19 October 2019 at 12:37 pm.

The identifier subset is composed of identity labels corresponding to each data in the dataset, which is defined as :

$$ID_{(p \cdot s) \times 1} = \{id_i\} \tag{5}$$

Among them, id_i is the identity label corresponding to the i -th fingerprint. Each data in the dataset has a unique identity label corresponding to it. Figure 5 shows an example of identifier.

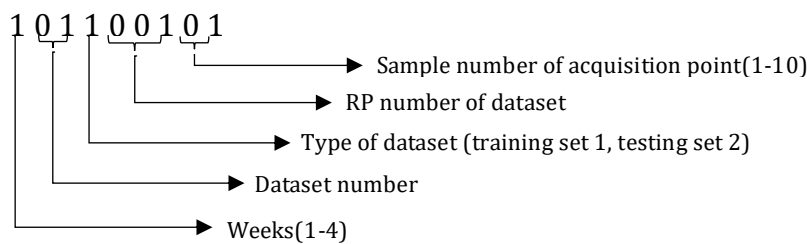


Figure 5 Examples of data identifiers

The dataset is stored as a file, organized by the acquisition area and time, and stored separately in different folders. For each data subset $D_{(m,k,n)}$, there are four csv files that store RSS, coordinates, time and identifier subsets. The types of datasets ('trn' represents the training set, 'tst' represents the testing set), acquisition weeks and data subset types ('rss', 'crd', 'tms' and 'ids' represent RSS, coordinates, time and identifier sets respectively) are distinguished by file names. For example, the file '02 / tst01rss.csv' contains a RSS subset of the first testing set from the second acquisition week.

4. Characteristics analysis of datasets

This section mainly analyzes the RSS variation characteristics in the dataset, compares the influence of signal frequency band on positioning and the positioning accuracy of different positioning methods on the dataset in this paper. In this paper, We process the dataset, visualize the variation characteristics of the signal and the positioning error, clearly and intuitively show the characteristics of the signal in this dataset.

4.1. RSS variation characteristics

In order to analyze and compare the signal strength and stability at RP, this paper visualizes some data in the dataset. Figure 6 shows the RSS value and mean square deviation of 2.4G signal from AP3 collected at each RP of $D_{(1,1,01)}$ (the first training set in the first week of the gate channel region) of DB₁. AP₃ coordinates (26.968 m, 53.439 m, 2 m) in the upper left corner of the figure. The height and color of the rectangular column in the figure correspond to the RSS collected at RP, and the length of the rectangular column is the mean square deviation of RSS. It can be seen from Figure 6 that the closer the AP₃ is, the stronger the RSS is and the more

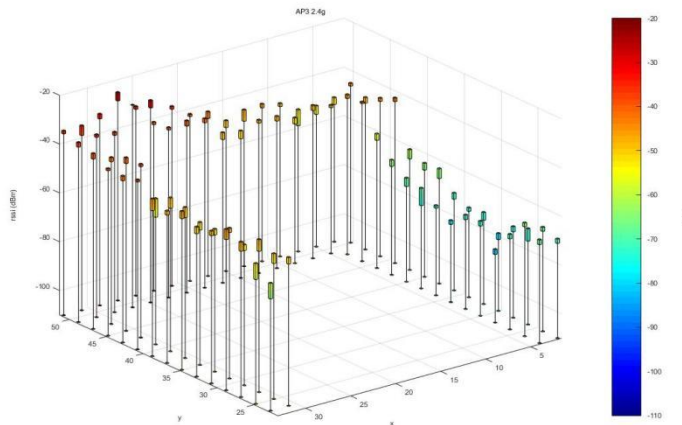


Figure 6 Mean and mean square deviation of 2.4G signal strength of AP3 in gate channel region

stable the signal is, but the signal fluctuation of several RPs closest to the AP₃ becomes larger. At the right RP of the figure, the RSS of the signal has a sudden change, which is mainly due to the blocking of the concrete wall in the middle of the site, resulting in signal attenuation. It is obvious that the environmental structure has a great influence on WiFi signal.

4.2. Characteristics of signals in different frequency bands

The signal has different propagation rules in different frequency bands. From the principle of signal propagation, under ideal conditions, the signal of different frequency bands, the side with the higher frequency propagates faster, but it is easy to attenuate, and the impact of obstructions is more serious; The low frequency side has strong signal penetrability and is not easily affected by the environment, but the signal strength itself does not change significantly.

In order to compare the characteristics and differences of different signal bands in underground parking, this section visualizes the RSS mean value, mean square deviation and corresponding positioning error of the two signals, which is convenient for analysis and comparison.

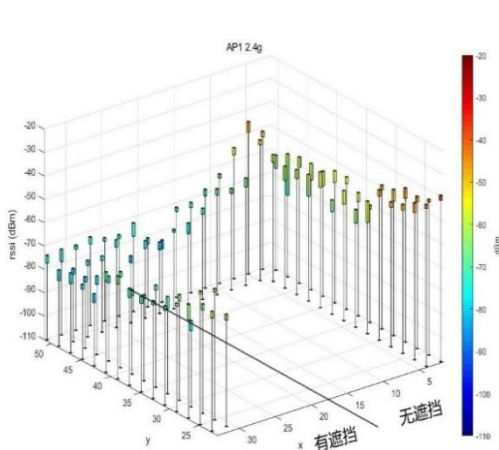


Figure 7(a) 2.4G signal RSS mean and variance

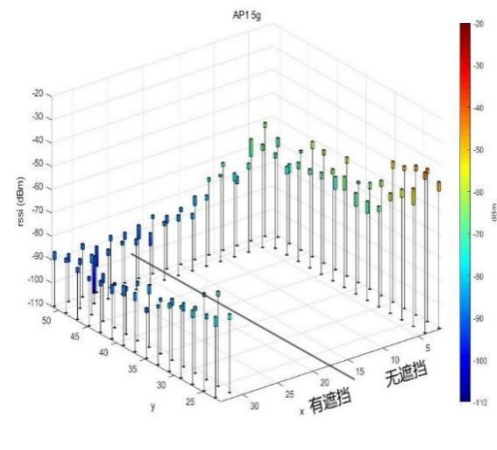


Figure 7(b) 5G signal RSS mean and variance

Figure 7 is the RSS mean value and mean square deviation of 2.4G signal and 5G signal at each RP of the gate channel area, which are RSS of AP₁. From these two figures, it can be seen that on the unshielded side, the variation of 5G signal is more obvious than that of 2.4G signal, and on the occluded side, the RSS mean of 2.4G signal is higher than that of 5G signal. It shows that 2.4G signal has stronger propagation ability in the space with obstruction, and 5G signal is more sensitive to the environment and distance.

Figure 8 is the positioning results obtained by kNN algorithm with $k = 9$ in two regions using 2.4G signal, 5G signal and mixed use of two signals. The transverse axis is positioning error, and the longitudinal axis is the proportion of positioning error in all positioning results. In the graph, point lines correspond to 2.4G, point virtual lines correspond to 5G, real lines correspond to mixed signals, and yellow virtual lines represent 75 % of the error.

Figure 8 (a) shows the positioning results of $D_{(1,2,1)}$ of DB₁. It can be found that in the gate channel area, the positioning effect of 2.4G is better than 5G, and the error value corresponding to 75% error is about 3 to 4 meters. Figure 8 (b) shows the positioning results of $D_{(1, 2, 1)}$ of DB₂. It can be found that in the parking area, the positioning effect of 5G signal is better than 2.4G signal, and the error value corresponding to 75% error is about 6 to 7 meters.

According to the results in Figure 7 and Figure 8, combined with the environmental characteristics of the underground parking, it can be found that since the middle part of the gate channel area is all cement wall, the 5G signal is more likely to attenuate when propagating, So the positioning accuracy of 2.4G signal is higher. In the parking area, the RSS of each AP is strong, the difference of fingerprints is small, and the environment of the parking area is complex. A large number of vehicles make the signal propagation uncertain and unstable, which has a great influence on the positioning accuracy. The final positioning result is worse than that of the gate channel area. Without the barrier of concrete wall, the 5G signal is more obvious for the change of distance, and the positioning accuracy of 5G signal in the parking area is higher.

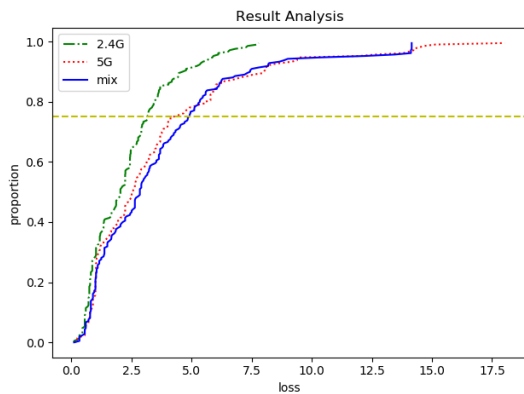


Figure 8 (a) Location error of different signals in the gate channel region

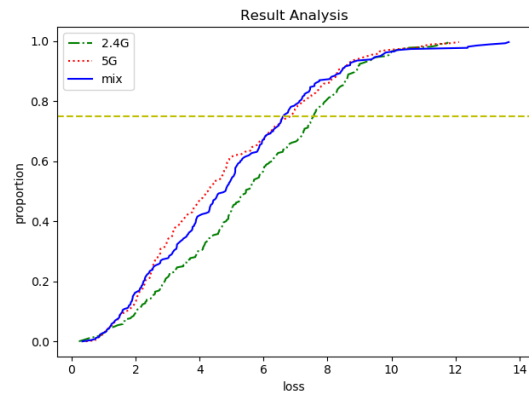


Figure 8(b) Location error of different signals in parking area

4.3. Comparison of positioning effects of different algorithms

In order to test the positioning effect of the dataset and the applicability of different positioning methods, this section uses six commonly used indoor positioning methods for positioning, and analyzes and compares the positioning accuracy. The parameters required in some algorithms are taken as the parameter values by transverse comparison, with the best positioning effect. These six methods are :

1.Prob: This is the first probabilistic method proposed by Youssef and Agrawala^[24], It finds the position $X(x, y, z)$ from the training set to maximize the probability of $P(X|s)$, and s is the fingerprint of the target position. According to Bayesian theorem $argmax_X [P(X|s)] \approx argmax_X [P(s|X)]$, but $P(s|X) = \prod P(s_i|X)$, where s_i is the RSS component corresponding to the i th AP in fingerprint s . According to the analysis in Berkvens^[25], the calculation method of $P(s_i|X)$ is as follows :

$$P(s_i|X) = \int_{s_i-0.5dBm}^{s_i+0.5dBm} N(\mu_i, \sigma^2_i) dw \quad (6)$$

Where w is the variable in the RSS domain, $N(\mu_i, \sigma^2_i)$ is the normal distribution, and μ_i and σ^2_i are the RSS mean and variance of the i th AP in the fingerprint group collected on position X . 1 dBm is the typical measurement accuracy of WiFi signal measurement, so the positive and negative 0.5 dBm is taken as the integral interval.

2.kNN: This is the first method proposed by Bahl and Padmanabhan^[26] to find k fingerprints closest to the current fingerprint in the dataset. The predicted target position is estimated to be the position of the nearest k fingerprint centroid. We set k to 9 and calculate it with Euclidean distance as fingerprint distance.

3.WkNN: This method is an improved algorithm based on kNN method. After finding k fingerprints closest to the current fingerprint in the fingerprint space, each fingerprint weight is given according to the calculated error, and the centroid of the fingerprint given weight is used as the position estimation value. The value of k in the algorithm is also 9, which is calculated using Euclidean distance.

4.Stg: This method first screens the fingerprints^[27], and some APs contain s strongest RSS components. The fingerprints with these AP signals are selected to match the fingerprints to be tested. For the selected fingerprints, the calculation will continue using the kNN method described earlier. This article sets $s = 3, k = 5$.

5.Gk: The algorithm is based on parametric modeling of logarithmic RSS random process, which obeys normal distribution. Each RSS is considered to be the mean value, and the standard deviation is set to a constant of all observed values. It calculates the possibility of RSS values at each fingerprint position and estimates the position by mean of the highest likelihood values. Roos^[28] et al. first used the method as a kernel density estimator (KDE) for WiFi-RSS-based positioning.

6.SVM: The algorithm is a classification algorithm based on support vector machine model, through the training set of fingerprint and coordinate data training model, so as to predict the testing set fingerprint corresponding coordinates. Since the predicted coordinates can be regarded as a multi-classification problem, the improved multi-class support vector machine is mainly used in the positioning process, and the linear kernel is used as the kernel function of the vector machine.

In this paper, the first training set per week is used as the training data, and the data of the weekly testing set are tested respectively. In Figure 9, the 75 % positioning error curves of kNN, WkNN and Gk methods for 4 weeks are drawn. It can be seen from the figure that the positioning errors of WkNN and kNN algorithms are basically the same. Compared with other methods, the Gk method has the best positioning effect in a few weeks. The SVM algorithm is based on the dichotomy method. The data amount of a single point is quite different from that of the entire training set, and the positioning result is poor.

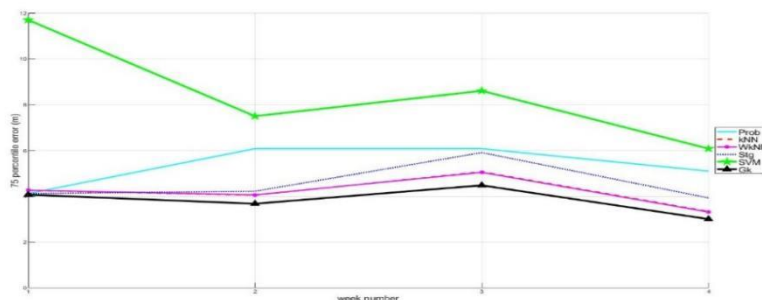


Figure 9 positioning results of six algorithms

5. Discussion and summary

In this paper, a multi-dimensional WiFi signal fingerprint dataset of underground parking is established to study the signal characteristics in underground parking environment and the characteristics of different frequency bands. The dataset collected 10 consecutive fingerprints at each position for a total of 4 weeks, which can be used to analyze short-term and long-term RSS changes and capture signal features at different frequencies. Weekly fingerprint data are organized as training sets and testing sets to analyze and compare the positioning effects of different fingerprint positioning methods. Other data can also be obtained by analyzing the time labels associated with each fingerprint data in the dataset. For example, the traffic flow data in the region can be analyzed by associating the RSS of the data with the acquisition time.

It takes a lot of effort to build a multi-dimensional WiFi signal fingerprint big dataset. Collectors spend at least eight hours a week to complete the acquisition task. When the label quality requirements are high, the larger area cannot use this acquisition scheme. Therefore, how to collect high-quality data is one of the main challenges of fingerprint positioning. Nowadays, the mainstream alternative methods, such as the method of Artificially generating simulation datasets according to signal characteristics, cannot guarantee the authenticity of the required data. Crowdsourcing / collaborative fingerprint acquisition scheme cannot guarantee the high quality of the required data. In a crowded environment, neither of these two methods may be

able to repeatedly collect fingerprints at the same position. If label quality is not taken into account, it is recommended to build datasets using manual generation and crowdsourcing / collaboration methods.

References

- [1] Li Qingquan, ZHOU Baoding, MA Wei, et al. Research process of GIS-Aided indoor localization[J]. *Acta Geodaetica et Cartographica Sinica*, 2019, 48(12): 1498-1506. DOI:10.11947/j.AGCS.2019.20190455
- [2] GAO Weiguang, MIAO Weikai, CHEN Gucang, JIA Song. Evaluation and analysis of stochastic modeling of BeiDou GEO/IGSO/MEO satellite observation[J]. *Acta Geodaetica et Cartographica Sinica*, 2020, 49(12):1511-1522
- [3] Alarifi, A.; Al-Salman, A.; Alsaleh, M.; Alnafessah, A.; Al-Hadhrami, S.; Al-Ammar, M.A.; Al-Khalifa, H.S. Ultra Wideband Indoor Positioning Technologies: Analysis and Recent Advances[J]. *Sensors*, 2016, 16(5), 707.
- [4] Jimenez, A.; Seco, F. Comparing Ubisense, Bespoon and Decawave UWB location systems: Indoor performance analysis[J]. *IEEE Trans. Instrum. Meas.* 2017, 66, 2106-2117.
- [5] ZHANG YaLei, WANG Jian, HAN HouZeng, YANG Deng. Research and precision analysis of indoor ranging model based on Bluetooth[J]. *Science of Surveying and Mapping*. 2020, <https://kns.cnki.net/kcms/detail/11.4415.P.20201125.1837.034.html>.
- [6] Seco F, Jimenez A.R, Zampella F. Fine-Grained Acoustic Positioning with Compensation of CDMA Interference[C]. In *Proceedings of the 2015 IEEE International Conference on Industrial Technology (ICIT)*, 2015, 3418-3423.
- [7] Hou, Y.; Xiao, S.; Bi, M.; Xue, Y.; Pan, W.; Hu, W. Single LED Beacon-Based 3-D Indoor Positioning Using Off-the-Shelf Devices[J]. *IEEE Photonics J.* 2016, 8, 1-11.
- [8] YANG Zheng, XU Jingao, YAO Lina. Indoor localization: Challenges and opportunities[J]. *Journal of Northwest University(Natural Science Edition)*, 2018, 48(2):172-182.
- [9] Torres-Sospedra, J.; Jiménez, A.R.; Knauth, S.; Moreira, A.; Beer, Y.; Fetzer, T.; Ta, V.C.; Montoliu, R.; Seco, F.; Mendoza-Silva, G.M.; et al. The Smartphone-Based Offline Indoor Location Competition at IPIN 2016: Analysis and Future Work[R]. *Sensors* 2017, 17(3), 557.
- [10] SHAN Jie. Remote Sensing: From Trained Professional to General Public[J]. *Acta Geodaetica et Cartographica Sinica*, 2017, 46(10):1434-1446
- [11] Torres-Sospedra J, Montoliu R, Martínez-Usó A, Avariento J.P, Arnau T.J, Benedito-Bordonau M., Huerta J. UJIIndoorLoc: A new multi-building and multi-floor database for WLAN fingerprint-based indoor localization problems[C]. In *Proceedings of the 2014 International Conference on Indoor Positioning and Indoor Navigation (IPIN)*, 2014, 261-270.
- [12] Lohan E.S, Torres-Sospedra J, Leppäkoski H, Richter P, Peng Z, Huerta J. Wi-Fi Crowdsourced Fingerprinting Dataset for Indoor Positioning[J]. *Data* 2017, 2(4):32.
- [13] Yang Jianghong, Zhao Xiaohu, Li Zan. Crowdsourcing Indoor Position by Light-Weight Automatic Fingerprint Updating via Ensemble Learning[J]. *IEEE Access*, 2019, 7:26255-26267.
- [14] Hossain A.K.M.M, Soh W.S. A survey of calibration-free indoor positioning systems. *Computer. Communications.* 2015, 66:1-13.
- [15] Wang B, Chen Q, Yang L.T, Chao H.C. Indoor smartphone localization via fingerprint crowdsourcing: challenges and approaches[J]. *IEEE Wireless Communications*, 2016, 23:82-89.
- [16] Gu Y, Chen M, Ren F, Li J. HED: Handling environmental dynamics in indoor WiFi fingerprint localization[C]. *2016 IEEE Wireless Communications and Networking Conference*, 2016, 1-6.
- [17] Hayashi T, Taniuchi D, Korpela J, Maekawa T. Spatio-temporal adaptive indoor positioning using an ensemble approach[J]. *Pervasive Mob. Computer* 2017, 41:319-332.
- [18] Barsocchi P, Crivello A, La Rosa D, Palumbo F. A multisource and multivariate dataset for indoor localization methods based on WLAN and geo-magnetic field fingerprinting[C]. *2016 International Conference on Indoor Positioning and Indoor Navigation (IPIN)*, 2016, 1-8.
- [19] Popleteev A. AmbiLoc: A year-long dataset of FM, TV and GSM fingerprints for ambient indoor localization[C]. *2017 International Conference on Indoor Positioning and Indoor Navigation (IPIN)*, 2017, 18-21.

- [20] Kasebzadeh P, Hendeby G, Fritsche C, Gunnarsson F, Gustafsson F. IMU Dataset For Motion and Device Mode Classification[C]. 2017 International Conference on Indoor Positioning and Indoor Navigation (IPIN), 2017, 1-8.
- [21] Hanley D, Faustino A, Zelman S, Degenhardt D, Bretl T. MagPIE: A Dataset for Indoor Positioning with Magnetic Anomalies[C]. 2017 International Conference on Indoor Positioning and Indoor Navigation (IPIN), 2017, 1-8.
- [22] Montoliu R, Sansano E, Torres-Sospedra J, Belmonte O. IndoorLoc Platform: A Public Repository for Comparing and Evaluating Indoor Positioning Systems[C]. 2017 International Conference on Indoor Positioning and Indoor Navigation (IPIN), 2017, 18-21.
- [23] German Martin Mendoza Silva, Joaquín Torres-Sospedra, Elena Simona Lohan, Joaquín Huerta. Long-Term WiFi Fingerprinting Dataset for Research on Robust Indoor Positioning[J]. Data Descriptor, 2018, 3(3):1-17
- [24] Bogdandy B. WiFi RSSI preprocessing library for Android[C]. ICC, 2018, 19th:28-31
- [25] Berkvens R, Peremans H, Wey M. Conditional Entropy and Location Error in Indoor Localization Using Probabilistic Wi-Fi Fingerprinting[J]. Sensors 2016, 16(10):1636.
- [26] Yanling Lu, Di Zhang. An Improved Method and Implementation of Indoor Position Fingerprint Matching Localization Based on WLAN[J]. Lecture Notes in Computer Science (LNCS 11354), 2019, 638-649.
- [27] Marques N, Meneses F, Moreira A. Combining similarity functions and majority rules for multi-building, multi-floor, WiFi positioning[C]. 2012 International Conference on Indoor Positioning and Indoor Navigation (IPIN), 2012, 1-9.
- [28] Tong Li, Ai S, Tateno S. Comparison of Multilateration Methods Using RSSI for Indoor Positioning System[C]. Annual Conference of the Society of Instrument and Control Engineers of Japan (SICE), 2019, 58th:371-375.

Author: Che Ronghua, born in March 1979, female, Liao Cheng Infant Normal School, lecturer, master's degree, research direction is computer software technology.